Composites Science and Technology 167 (2018) 126–133

Contents lists available at ScienceDirect

Composites Science and Technology

journal homepage: www.elsevier.com/locate/compscitech

Thinner and better: (Ultra-)low grammage bacterial cellulose nanopaper-reinforced polylactide composite laminates

Martin Hervy[a], Frederic Bock[a,b], Koon-Yang Lee[a,*]

[a] Department of Aeronautics, Imperial College London, South Kensington Campus, SW7 2AZ, London, United Kingdom
[b] Institute of Polymer and Composites, Hamburg University of Technology, Denickestrasse 15, D-21073, Hamburg, Germany

ARTICLE INFO

Keywords:
Laminate
Nano composites
Polymer-matrix composites (PMCs)
Mechanical properties
Nanocellulose

ABSTRACT

One of the rate-limiting steps in the large-scale production of cellulose nanopaper-reinforced polymer composites is the time consuming dewatering step to produce the reinforcing cellulose nanopapers. In this work, we show that the dewatering time of bacterial cellulose (BC)-in-water suspension can be reduced by reducing the grammage of BC nanopaper to be produced. The influence of BC nanopaper grammage on the tensile properties of BC nanopaper-reinforced polylactide (PLLA) composites is also investigated in this work. BC nanopaper with grammages of 5, 10, 25 and 50 g m^{-2} were produced and it was found that reducing the grammage of BC nanopaper from 50 g m^{-2} to 5 g m^{-2} led to a three-fold reduction in the dewatering time of BC-in-water suspension. The porosity of the BC nanopapers, however, increased with decreasing BC nanopaper grammage. While the tensile properties of BC nanopapers were found to decrease with decreasing BC nanopaper grammage, no significant difference in the reinforcing ability of BC nanopaper with different grammages for PLLA was observed. All PLLA composite laminates reinforced with BC nanopapers possessed similar tensile modulus of 10.5–11.8 GPa and tensile strength of 95–111 MPa, respectively, at a BC loading fraction $v_{f,BC}$ = 39–53 vol.-%, independent of the grammage and tensile properties of the reinforcing BC nanopaper.

1. Introduction

Cellulosic fibres in the nanometre scale, more commonly known as nanocellulose, is a family high performance bio-based nanofibres with tensile moduli and strengths estimated to be 100–160 GPa and 0.3–22 GPa, respectively [1,2]. Nanocellulose possesses the combined properties of cellulose, e.g. broad chemical modification capacity [3] and high crystallinity (up to 80% for cellulose nanocrystals) [4], with the features of a nano-material [5], e.g. high surface energy (~65 mJ m^{-2}) [6] and high specific surface area (up to 605 m^2 g^{-1} [7]). Nanocellulose is also a lightweight material (~1.5 g cm^{-3}) that is abundant in nature. Thus, nanocellulose is often explored as nano-reinforcement for polymers.

Nanocellulose can be obtained via two approaches: top-down or bottom-up. In the top-down approach, woody biomass such as wood pulp is passed through high-pressure homogenisers [8,9], microfluidisers [10] or stone grinders [11] to liberate the elementary microfibrils from the micrometre-sized pulp fibres [12]. Wood-derived nanocellulose is more commonly known as nanofibrillated cellulose (NFC). The bottom-up approach, on the other hand, utilises cellulose-producing bacteria, such as *Komagataeibacter* to convert low molecular weight sugars to nanocellulose [13]. These microbially-synthesised nanocellulose, also known as bacterial cellulose (BC), is an ultrapure form of nanocellulose without impurities such as hemicellulose or traces of lignin that are often present in NFC [14].

A method to efficiently utilise nanocellulose as reinforcement for advanced composite applications is to exploit the reinforcing ability of a dried and well-consolidated nanocellulose network, e.g. a 2-D reinforcement in the form of cellulose nanopaper. Henriksson et al. [15] fabricated NFC nanopaper-reinforced melamine formaldehyde (MF) composites by immersing a single sheet of reinforcing NFC nanopaper in a water/MF solution, followed by drying and crosslinking. The authors obtained a tensile modulus and strength of 15.7 GPa and 108 MPa, respectively, for NFC nanopaper-reinforced MF composites with a nanocellulose loading of 87 wt.-%. NFC nanopaper has also been incorporated into epoxy resin using vacuum assisted resin infusion [16]. At a nanocellulose loading of 40 vol.-%, the resulting NFC nanopaper-reinforced epoxy composites possessed a tensile modulus and strength of 7.1 GPa and 103 MPa, respectively.

In addition to NFC nanopaper, BC nanopaper has also been exploited as 2-D reinforcement for polymers. Nakagaito et al. [17] fabricated BC nanopaper-reinforced phenol formaldehyde (PF)

* Corresponding author.
E-mail address: koonyang.lee@imperial.ac.uk (K.-Y. Lee).

https://doi.org/10.1016/j.compscitech.2018.07.027
Received 6 March 2018; Received in revised form 22 June 2018; Accepted 18 July 2018
Available online 24 July 2018

composites by first immersing dried and well-consolidated sheets of BC nanopaper in PF resin diluted with methanol [17]. The PF-impregnated BC nanopapers (25 sheets in total) were then air-dried, stacked and heat consolidated to produce the BC nanopaper-reinforced PF composites. Bending modulus and strength as high as ~20 GPa and ~350 MPa, respectively, have been obtained for composites containing BC nanopaper loading of 88 wt.-%. A simpler approach to produce BC nanopaper-reinforced polymer composites was presented by Montrikittiphant et al. [18], whereby the authors sandwiched a sheet of BC nanopaper between two thin polylactide films and heat consolidated the layup. The resulting BC nanopaper-reinforced polylactide was found to possess a tensile modulus and strength of 6.9 GPa and 125 MPa, respectively, for a BC nanopaper loading of 65 vol.-%.

While it is evident that both BC and NFC nanopapers serve as excellent 2-D reinforcement for polymers, the rate-limiting step towards the large-scale production of these high-performance cellulose nanopaper-reinforced polymer composites is the time-consuming dewatering step to produce the reinforcing cellulose nanopaper. Cellulose nanopaper is typically produced by first creating a suspension of nanocellulose-in-water at a consistency of ~0.1–0.5 wt.-%. The nanocellulose-in-water suspension is then dewatered using vacuum-assisted or gravity-driven filtration, followed by heat consolidation. We have previously found that the dewatering time of BC and NFC suspensions to produce 60 g m^{-2} nanopaper was 5 min and 40 min, respectively [19]. Some authors reported dewatering times as low as 10 min and as high as 3–4 h for NFC suspensions [20,21]. The dewatering time of NFC suspension is often longer than BC suspension because NFC forms a more homogeneous suspension in water, whilst aggregates or bundles of BC is often observed due to difficulties in disrupting the three-dimensional nanofibrous network of BC pellicles using low energy blending [22]. The aggregates or bundles of BC possess higher hydrodynamic diameter, which led to higher settling velocity compared to NFC, reducing the dewatering time of BC suspension. Furthermore, NFC typically contains significant amount of hemicellulose, which has high water holding capacity that also contributes to longer dewatering time.

The dewatering time of a pulp suspension to produce conventional papers, on the other hand, is typically less than 2 min [23]. A new strategy is therefore needed to reduce the dewatering time of nanocellulose suspension for the large-scale manufacturing of high performance cellulose nanopaper-reinforced polymers. In this work, we report the production of (ultra-)low grammage BC nanopaper as a mean to reduce the dewatering time of nanocellulose suspension. Model BC nanopaper with grammages of 5, 10, 25 and 50 g m^{-2} were produced and the influences of BC nanopaper grammage on the dewatering time, as well as mechanical properties are investigated. The reinforcing ability of (ultra-)low grammage BC nanopapers for polylactide is also discussed in this work.

2. Experimental section

2.1. Materials

Poly(L-lactic acid) (PLLA) (L9000, molecular weight ≥ 150 kDa, D-content ≈ 1.5%) was purchased from Biomer GmbH and used as the matrix for the production of BC nanopaper-reinforced PLLA composites. Sodium hydroxide (pellets, purity > 98.5%) was purchased from VWR International (Lutterworth, UK). 1,4-Dioxane (ACS Reagent, purity ≥ 99%) was purchased from Sigma-Aldrich (Gillingham, UK). These materials were used as received without further purification. BC in the form of commercially available nata de coco (coconut gel in syrup) with 97.5 wt.-% water content was purchased from a retailer (Xiangsun Ltd, Lugang Township, Changhua County, Taiwan).

2.2. Purification of BC from nata de coco

The purification of BC from nata de coco has been described in our previous work [22]. Briefly, 150 g of nata de coco cubes were added to 3.5 L of de-ionised water and heated to 80 °C under magnetic stirring. 14 g of NaOH pellets were then added into this dispersion and left to stir at 80 °C for 2 h. After this purification step, the dispersion was poured onto a metal sieve (mesh size = 300 μm) to recover the purified nata de coco cubes. The cubes were then rinsed with 5 L of de-ionised water prior to blending (Breville VBL065) in another 5 L of de-ionised water for 2 min to create a homogeneous suspension of BC-in-water. The suspension was centrifuged (SIGMA 4-16S, SciQuip Ltd., Newton, UK) at 6800 × g and the excess water was removed. This blending-centrifugation step was repeated until neutral pH was attained. The final consistency of the BC-in-water suspension was adjusted to 2 wt.-% by centrifugation prior to storage for subsequent use.

2.3. Manufacturing of BC nanopaper with different grammages

BC nanopaper with grammages of 5, 10, 25 and 50 g m^{-2} were produced in this work. To prepare BC nanopaper with the desired grammage, an equivalent amount of the previously purified BC-in-water was first dispersed in 500 mL of de-ionised water using a blender (Breville VBL065). This BC-in-water suspension was then vacuum filtered onto a 12 cm diameter woven polyester peel ply (AeroFilm® PP180, 85 g m^{-2}, Easy Composites Ltd., Staffordshire, UK) placed on top of a filter paper (Grade 413, 5–13 μm particle retention, VWR International Ltd., Lutterworth, UK) in a Büchner funnel. The function of the polyester peel ply was to aid the subsequent processing of the wet BC filter cake. Without the polyester peel ply, the wet BC filter cakes used to produce 5 g m^{-2} and 10 g m^{-2} BC nanopapers were too fragile to be removed directly from the used filter paper for subsequent processing.

After the filtration step, the polyester peel ply with the wet BC filter cake still on top was carefully separated from the used filter paper and wet pressed between fresh filter and blotting papers (Grade 3MM CHR, VWR international Ltd, Lutterworth, UK) under a weight of 10 kg for 10 min to absorb the excess water. This wet pressing step was repeated twice, with fresh filter and blotting papers used everytime. A final heat consolidation step was then performed in a hydraulic hot press (4122 CE, Carver Inc., Wabash, IN, USA) using a compaction force of 1 t at 120 °C for 30 min to further dry and consolidate the BC filter cake into nanopaper. Once the nanopaper had cooled to room temperature, it was then carefully separated from the polyester peel ply. All BC nanopapers manufactured were stored in a sealed environment containing silica gel pouches to keep the nanopapers dry.

2.4. Fabrication of BC nanopaper-reinforced PLLA composite laminates

BC nanopaper-reinforced PLLA composite laminates were produced using film-stacking method. The stacking sequences of BC nanopaper with different grammages and PLLA are shown in Fig. 1. These stacking sequences were chosen such that the overall grammage of the BC nanopaper(s) within the composite laminates was kept constant at 50 g m^{-2}. Prior to producing the composite laminates, thin PLLA films were produced by solution casting. Briefly, PLLA pellets were dissolved in 1,4-dioxane at a mass ratio of 1:12 at 65 °C overnight under magnetic stirring. Once the polymer solution was cooled to room temperature, it was then casted onto a toughened glass plate using an automated film applicator (Elcometer 4340, Elcometer Ltd., Manchester, UK) and the solvent was evaporated to produce the thin PLLA film. The speed of the casting knife was set to be 5 mm s^{-1}.

The fabricated BC nanopaper(s) and PLLA films were then stacked in accordance to the stacking sequences shown in Fig. 1 and sandwiched between two heat-resistant non-stick polyimide films (UPILEX®, Goodfellow Cambridge Ltd., Huntingdon, UK). The lay-up was pre-heated in a hydraulic hot press (4122 CE, Carver Inc., Wabash, IN, USA) to 180 °C for 3 min, followed by a consolidation step at the same temperature for 2 min using a compaction force of 1 t. Model BC

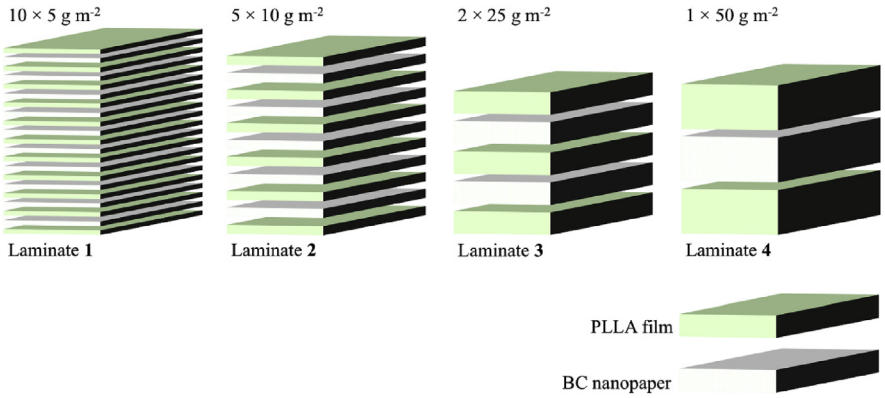

Fig. 1. The stacking sequences of the BC nanopaper-reinforced PLLA composite laminates fabricated in this work. Laminate **1** possessed 10 sheets of 5 g m^{-2} BC nanopaper; Laminate **2** possessed 5 sheets of 10 g m^{-2} BC nanopaper; Laminate **3** possessed 2 sheets of 25 g m^{-2} BC nanopaper; Laminate **4** possessed 1 sheet of 50 g m^{-2} BC nanopaper, respectively.

nanopaper-reinforced PLLA composite laminates reinforced with 10 × 5 g m^{-2}, 5 × 10 g m^{-2}, 2 × 25 g m^{-2} and 1 × 50 g m^{-2} BC nanopaper (s) are herein termed Laminate **1**, Laminate **2**, Laminate **3** and Laminate **4**, respectively. All composite laminates were stored in a sealed environment containing silica gel pouches to keep the composite laminates dry prior to subsequent characterisation. As a control, neat PLLA film was also produced by hot pressing PLLA pellets directly at a temperature of 180 °C using a compaction force of 1 t for 2 min.

2.5. Characterisation of BC nanopapers and their respective model PLLA composites

The internal morphology of the BC nanopapers and the model BC nanopaper-reinforced PLLA composite laminates was investigated using a large chamber SEM (S-3700N, Hitachi, Tokyo, Japan) operated at an accelerating voltage of 10 kV. Prior to SEM, the tensile fractured specimens were attached onto aluminium stubs using carbon tabs and Au coated (Agar auto sputter coater, Agar Scientific, Stansted, UK) at 40 mA for 20 s.

The envelope density (ρ_e) of the BC nanopapers and the manufactured model composite laminates was calculated by taking the ratio between the mass and the envelope volume of the specimen. The porosity of the BC nanopapers ($P_{\text{BC nanopaper}}$) was then calculated using:

$$P_{\text{BC nanopaper}}(\%) = \left(1 - \frac{\rho_e}{\rho_f}\right) \times 100 \quad (1)$$

where ρ_f is the absolute density of BC nanofibres, measured to be 1.51 ± 0.02 g cm^{-3} using He pycnometry (Accupyc II 1340 Micromeritics Ltd., Hexton, UK) [22]. To calculate the porosity of the model BC nanopaper-reinforced PLLA composite laminates ($P_{\text{composites}}$), the void free density of the laminates ($\rho_{c,\text{ void free}}$) was first calculated from the measured weight fraction of BC ($w_{f,BC}$) within the composite laminates using:

$$\rho_{c,\text{void free}} = \frac{1}{\frac{1 - w_{f,BC}}{\rho_m} + \frac{w_{f,BC}}{\rho_f}} \quad (2)$$

where ρ_m is the absolute density of neat PLLA, measured to be 1.26 ± 0.01 g cm^{-3} using He pycnometry. The porosity of the model BC nanopaper-reinforced PLLA composite laminates ($P_{\text{composites}}$) was then calculated from:

$$P_{\text{composites}}(\%) = \left(1 - \frac{\rho_e}{\rho_c}\right) \times 100 \quad (3)$$

The tensile properties of BC nanopapers and the model BC nanopaper-reinforced PLLA composite laminates were characterised in accordance to BS EN ISO 527: 2012. Prior to the test, dog bone shape test specimens were cut using a manual cutting press (ZCP020, Zwick Testing Machines Ltd., Leominster, UK). The test specimens possessed an overall length of 35 mm, a gauge length of 10 mm and the narrowest part of the dog bone shape specimens has a width of 2 mm. To avoid damaging the gripping zone of the test specimens, which could potentially lead to earlier onset failure of the specimens, all test specimens were secured onto 140 g m^{-2} paper testing cards using two-part cold curing epoxy resin (Araldite 2011). Tensile tests were carried out using a micro-tensile tester (Model MT-200, Deben UK Ltd., Woolpit, UK) equipped with a 200 N load cell. A pair of dots was marked on the surface of each test specimen in the direction of load. The strain of the test specimen was then evaluated by monitoring the movement of these two dots using a non-contact optical extensometer (iMetrum Ltd., Bristol, UK). All tensile tests were conducted using a crosshead displacement speed of 0.2 mm min^{-1}, which corresponded to a test specimen strain rate of 2 × 10^{-4} s^{-1}. The temperature and relative humidity during the test were measured to be 21 °C and 50%, respectively. The reported tensile properties were averaged over 5 test specimens.

3. Results and discussion

3.1. Dewatering time of the BC-in-water suspensions

The dewatering time of BC-in-water suspensions to produce BC nanopaper with grammages of 5, 10, 25 and 50 g m^{-2} is shown in Fig. 2. It can be seen from this figure that the lower the grammage of BC nanopaper to be produced, the faster the dewatering time of the BC-in-water suspension. At the start of the dewatering process, BC nanofibres are deposited onto the filter medium (in this study, the filter medium used was a polyester peel ply placed on top of a filter paper) as a thin layer of BC nanofibre network. As dewatering progresses, the BC nanofibres deposit over the other on top of this thin layer of BC nanofibre network, forming a layered structure (see Fig. 3 for the SEM images

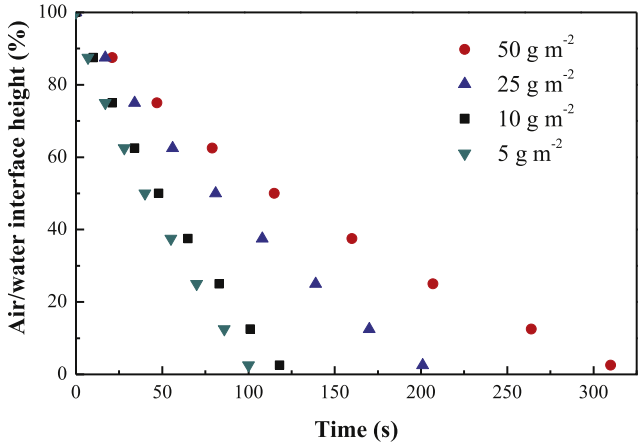

Fig. 2. Dewatering time of the BC-in-water suspensions to produce BC nanopaper with different grammages.

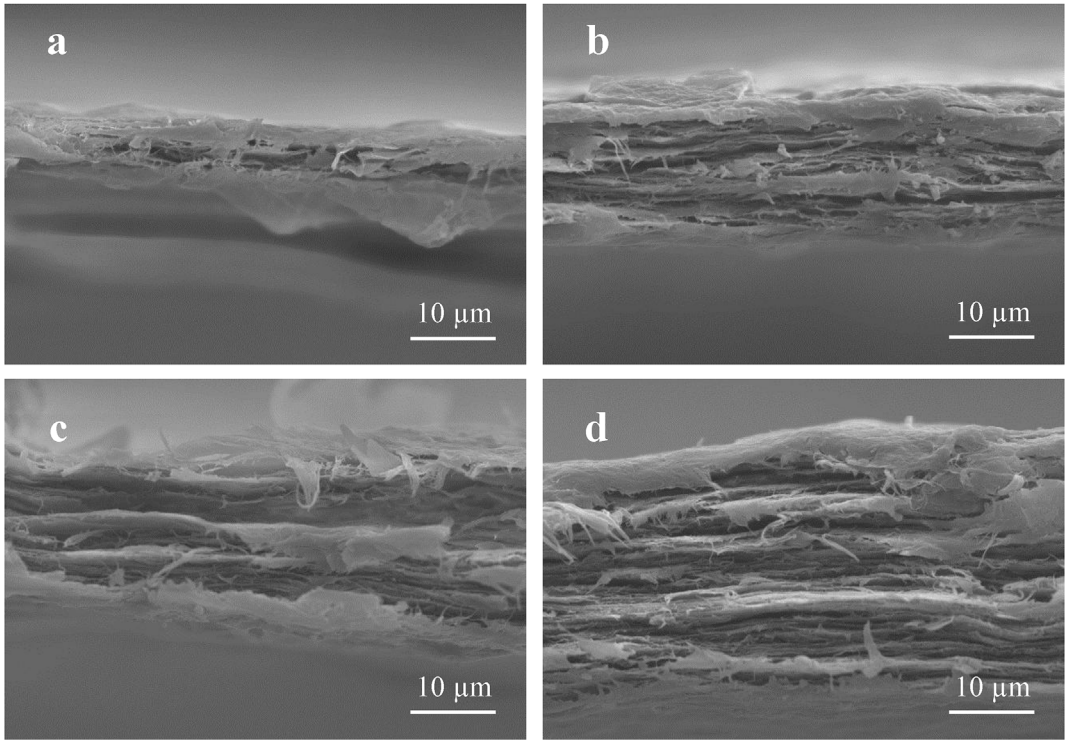

Fig. 3. Tensile fracture surfaces of (a) 5 g m^{-2}, (b) 10 g m^{-2}, (c) 25 g m^{-2} and (d) 50 g m^{-2} BC nanopaper, respectively, revealing the layered structure of BC nanopapers.

showing the internal morphology of fabricated BC nanopapers). Similar layered structure has also been observed by numerous researchers [24–26]. The build-up of the BC filter cake during the dewatering process leads to an increase in the flow resistance (e.g. a reduction in the permeability) of water through the filter cake. As a result, the dewatering time to produce a 5 g m^{-2} nanopaper, which has the thinnest filter cake, was significantly lower than the dewatering time to produce a 50 g m^{-2} BC nanopaper, which has the thickest filter cake.

3.2. Porosity of BC nanopaper at different grammages

The thickness and porosity of the fabricated BC nanopapers as a function of grammage are shown in Fig. 4. A 5 g m^{-2} BC nanopaper possessed a porosity of 78%. Increasing the BC nanopaper grammage to 50 g m^{-2} led to a progressive reduction in the porosity of the BC nanopaper to 48%. This reduction in porosity with increasing BC nanopaper grammage, which suggests better packing efficiency as the grammage increases, leads to the observed non-linearity of the thickness versus grammage plot (see Fig. 4).

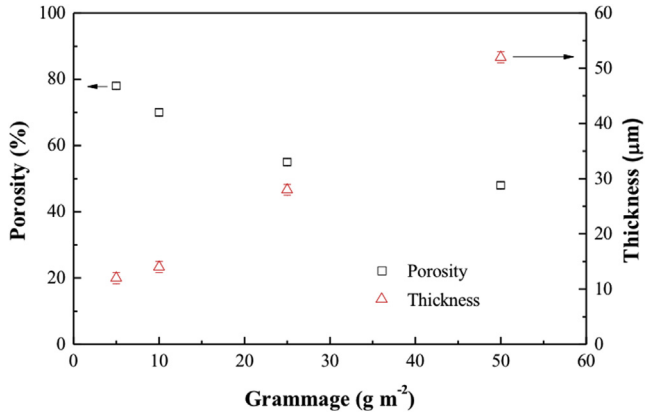

Fig. 4. Porosity and thickness of BC nanopapers as a function of grammage.

In addition to the dewatering time of BC-in-water suspension, another important step in the production of high load bearing capacity BC nanopaper is the shrinkage prevention of the wet BC filter cake during drying. If a cellulose fibre network is restrained from shrinkage, the slacks of the free fibre segments (e.g. exposed fibres within two fibre contact points) in the cellulose fibre network are removed, thereby improving the mechanical properties of the resulting dried cellulose fibre network [27]. This is also known as fibre segment activation. In this study, wet BC filter cake was restrained from shrinkage by applying a compaction force of 1 t during the heat consolidation step. The application of such high compaction force led to the slippage and repositioning of BC nanofibres, filling the voids within the wet BC filter cake, improving the packing efficiency and reducing the porosity of the resulting dried and well-consolidated BC nanopaper. This also corroborates with the moisture content of the wet BC filter cakes to produce BC nanopapers of different grammage at various stages of the nanopaper production (see Table 1).

Wet BC filter cake was found to possess a moisture content of approximately 78–88 wt.-% after the vacuum-assisted dewatering step prior to the first wet pressing step. However, the wet BC filter cakes to

Table 1
Moisture content of BC filter cake for different nanopaper grammage after each processing step.

BC filter cake	Moisture content (wt.-%)			
	50 g m^{-2}	25 g m^{-2}	10 g m^{-2}	5 g m^{-2}
After dewatering, prior to the 1st wet pressing step	88	86	85	78
After the 1st wet pressing step, prior to the 2nd wet pressing step	79	69	27	0
After the 2nd wet pressing step, prior to the heat consolidation step	66	24	0	0

produce 5 g m^{-2} and 10 g m^{-2} BC nanopapers dried after the first and second wet pressing steps, respectively, which used an applied compaction force of only 10 kg. The application of a compaction force of 1 t onto the already-dried 5 g m^{-2} and 10 g m^{-2} BC nanopapers in the heat consolidation step no longer leads to nanofibre slippage as irreversible hydrogen bonds have formed between the BC nanofibre (e.g. hornification). The BC filter cakes to produce 25 g m^{-2} and 50 g m^{-2} BC nanopapers, on the other hand, were found to possess significant higher moisture content even after the second wet pressing step. The application of 1 t compaction force on these BC filter cakes led to nanofibre slippage and void-filling. As a result, 25 g m^{-2} and 50 g m^{-2} BC nanopapers possessed lower porosity than 5 g m^{-2} and 10 g m^{-2} BC nanopapers. Due to the higher moisture content of BC filter cake to produce 50 g m^{-2} BC nanopaper, the effect of nanofibre slippage and hence void-filling is more pronounced. Consequently, 50 g m^{-2} BC nanopaper possessed lower porosity compared to 25 g m^{-2} BC nanopaper.

3.3. Tensile properties of BC nanopaper at different grammages

The representative stress-strain curves of the fabricated BC nanopaper at different grammages tested in uniaxial tension exhibited an initial elastic deformation, followed by inelastic deformation prior to catastrophic failure (see Fig. 5). The tensile modulus and strength of 5 g m^{-2} BC nanopaper were measured to be 2.4 GPa and 31 MPa, respectively (see Table 2). Increasing the grammage of BC nanopaper led to a progressive increase in tensile modulus and strength to 12.2 GPa and 134 MPa, respectively, for 50 g m^{-2} BC nanopaper. Similar trends have been observed for conventional paper made from micrometre-sized pulp fibres, whereby the tensile properties of paper increased with increasing paper grammage [28,29]. It can also be seen from Table 2 that both the specific tensile modulus and strength of BC nanopapers increased with increasing nanopaper grammage, suggesting that the differences in the porosity of the BC nanopapers is not the sole reason for the observed tensile properties variation.

The stress transfer efficiency of a 2-D random fibre network is related to its mean coverage ($\bar{c}$), defined as the expected number of fibres covering a point in the plane of support of the fibre network [30]. Mathematically, $\bar{c}$ is expressed as:

$$\bar{c} = \frac{\bar{\beta}\omega}{\delta} \tag{4}$$

where $\bar{\beta}$ denotes the grammage of the fibre network, ω denotes the fibre width and δ is the linear density of the fibre. The higher the value of $\bar{c}$, the better the stress transfer efficiency between the fibres in the 2-D random fibre network [31]. Since both ω and δ are identical for all nanopapers fabricated in this work, it can therefore be inferred from equation (4) that the higher the grammage, the higher the value of $\bar{c}$ and hence, better stress transfer between the BC nanofibres within the BC nanopaper. Furthermore, a reduction in the BC nanopaper grammage also leads to an increase in the relative amount of BC nanofibres between the surface and the bulk of the nanopaper. As the BC nanofibres on the surface are less efficient at transferring load [31], the (specific) tensile properties of the BC nanopapers also decrease with decreasing nanopaper grammage.

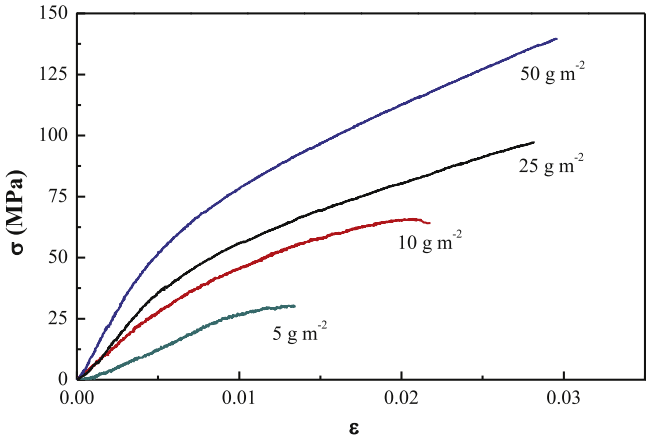

Fig. 5. Representative stress (σ) - strain (ε) curves of the BC nanopapers with different grammages loaded under uniaxial tension.

3.4. Tensile properties of model BC nanopaper-reinforced PLLA composite

Table 3 summarises the tensile properties of model BC nanopaper-reinforced PLLA composite laminates reinforced with 10 sheets of 5 g m^{-2} (Laminate **1**), 5 sheets of 10 g m^{-2} (Laminate **2**), 2 sheets of 25 g m^{-2} (Laminate **3**) and 1 sheet of 50 g m^{-2} (Laminate **4**) BC nanopaper(s), respectively. It can be seen from Table 3 that all BC nanopapers possessed excellent reinforcing ability for PLLA. Tensile moduli of between 10.5 and 11.8 GPa were obtained for model BC nanopaper-reinforced PLLA composite laminates at BC fibre volume fraction $v_{f,BC}$ = 39–53 vol.-%. The tensile strengths of the model BC nanopaper-reinforced PLLA composite laminates were measured to be between 95 and 111 MPa. The slight variation in the measured tensile properties between the model composite laminates can be attributed to the variation in $v_{f,BC}$ and porosity of the composites. By contrast, the tensile modulus and strength of neat PLLA were measured to be only 3.6 GPa and 57.5 MPa, respectively.

The fracture surfaces of the model BC nanopaper-reinforced PLLA composite laminates loaded under uniaxial tension are shown in Fig. 6. The observed internal morphology of the model composite laminates is consistent with the stacking sequences shown in Fig. 1, suggesting minimal bulk impregnation of the BC nanopaper(s) by molten PLLA, even though the grammage of the BC nanopaper was as low as 5 g m^{-2}. It has been previously shown that for cellulose nanopaper-reinforced polymer composites with such internal morphology, the tensile modulus and strength of the model composites should follow closely the prediction of the volume weighted average between the tensile properties of the cellulose nanopaper and the polymer matrix [1]:

$$E_c = E_{nanopaper} \times v_{f,BC} + E_{matrix} \times (1 - v_{f,BC}) \tag{5}$$

$$\sigma_c^* = \sigma_{nanopaper}^* \times v_{f,BC} + \sigma_{matrix}^* \times (1 - v_{f,BC}) \tag{6}$$

where E_c, $E_{nanopaper}$ and E_{matrix} denote the tensile modulus of the model composite, the reinforcing nanopaper and the polymer matrix, respectively. The term σ_c^* denotes the tensile strength of the model composites, $\sigma_{nanopaper}^*$ is the tensile strength of the cellulose nanopaper and σ_{matrix}^* is the tensile strength of the polymer matrix. Following equations (5) and (6), Laminate **1** should possess a tensile modulus of only 3.1 GPa and a tensile strength of only 47.5 MPa. However, the experimentally determined tensile properties showed otherwise. Laminate **1** was found to possess a tensile modulus and strength of 10.7 GPa and 95 MPa, respectively (see Table 3). In fact, significant positive deviation can be observed between the experimentally measured tensile properties and the rule-of-mixture predicted tensile properties (equations (5) and (6)) for all model BC nanopaper-reinforced PLLA composite laminates fabricated in this work (see Fig. 7). This discrepancy could be ascribed to the porosity of the composite laminates.

The porosity of Laminates **1–4** was found to be ~8–16% (see Table 3). However, the BC nanopapers fabricated in this work possessed porosities of between 48% and 78% (Fig. 4). Assuming that BC nanopapers are uniform rectangular slabs that are incompressible and impermeable to molten PLLA, the theoretical porosity of the model composite laminates ($P_{theoretical}$) is estimated to be between 33% and 58%. These values are significantly higher than the experimentally determined porosity values for the model BC nanopaper-reinforced PLLA composite laminates fabricated (see Table 3). Since cellulose nanopapers possess a rough surface [32], the porosity of a BC nanopaper can be

Table 2
Tensile modulus (E), tensile strength (σ^*), strain-at-break (ε^*), specific tensile modulus (E/ρ_e), specific tensile strength (σ^*/ρ_e) and work of fracture (U_T) of the fabricated BC nanopapers.

Sample	E [GPa]	σ^* [MPa]	ε^* [%]	E/ρ_e [GPa cm^3 g^{-1}]	σ^*/ρ_e [MPa cm^3 g^{-1}]	U_T[J m^{-3}]
5 g m^{-2}	2.4 ± 0.2	31 ± 3	1.9 ± 0.1	7.3 ± 1.2	91 ± 18	0.3 ± 0.1
10 g m^{-2}	5.0 ± 0.2	59 ± 2	2.3 ± 0.2	10.9 ± 1.8	128 ± 26	0.7 ± 0.1
25 g m^{-2}	8.9 ± 0.6	104 ± 3	3.2 ± 0.2	13.1 ± 2.2	153 ± 31	2.1 ± 0.1
50 g m^{-2}	12.2 ± 0.5	134 ± 3	3.0 ± 0.1	15.6 ± 2.6	172 ± 35	2.5 ± 0.1

Table 3
Tensile properties of BC nanopaper-reinforced composite laminates. Fibre volume fraction ($v_{f,BC}$), tensile modulus (E), tensile strength (σ^*) and strain-at-break (ε^*), envelop density (ρ_e), theoretical density ($\rho_{c,void\ free}$) and porosity ($P_{composites}$) the composites and neat PLLA.

Sample	$v_{f,BC}$ [%]	E [GPa]	σ^*[MPa]	ε^*[%]	ρ_e[g cm^{-3}]	$\rho_{c,void\ free}$[g cm^{-3}]	$P_{composites}$ [%]
PLLA	0	3.6 ± 0.1	57.5 ± 1.0	3.5 ± 0.4	1.26 ± 0.01	1.26 ± 0.01	0 ± 0
Laminate **1**	39 ± 3	10.7 ± 0.4	95.0 ± 0.9	2.2 ± 0.1	1.25 ± 0.07	1.36 ± 0.01	8 ± 1
Laminate **2**	48 ± 2	11.2 ± 0.4	102.4 ± 1.8	2.5 ± 0.1	1.23 ± 0.02	1.38 ± 0.01	11 ± 1
Laminate **3**	50 ± 3	10.5 ± 0.2	100.7 ± 1.9	3.0 ± 0.1	1.16 ± 0.01	1.39 ± 0.01	16 ± 1
Laminate **4**	53 ± 2	11.8 ± 0.2	111.4 ± 2.2	2.4 ± 0.1	1.28 ± 0.07	1.39 ± 0.01	8 ± 1

categorised into surface porosity and bulk porosity. It is postulated that during the heat consolidation step, the molten PLLA impregnated the surface porosity of the BC nanopapers, leading to composites with porosity lower than $P_{theoretical}$. These results also corroborated with the fracture surfaces of the model composites (Fig. 4), whereby no bulk impregnation of the BC nanopapers by PLLA was observed.

4. Concluding remarks

The large-scale production of cellulose nanopaper-reinforced polymer composites is often limited by the dewatering step to produce the reinforcing cellulose nanopaper. In this work, model (ultra-)low grammage BC nanopapers were produced as a mean to reduce the dewatering time of BC-in-water suspension and the reinforcing ability of (ultra-)low grammage BC nanopapers for PLLA was investigated. BC nanopaper with grammages of 5, 10, 25 and 50 g m^{-2} were produced and studied. It was found that reducing the grammage of BC nanopaper to be produced could significantly reduce the dewatering time of BC-in-water suspension, leading to faster production of BC nanopapers. The dewatering times to produce 5 g m^{-2}, 10 g m^{-2}, 25 g m^{-2} and 50 g m^{-2} BC nanopaper were measured to be 100 s, 118 s 201 s and 310 s, respectively. However, the porosity of the BC nanopapers was found to increase from 48% to 78% when the nanopaper grammage decreased from 50 to 5 g m^{-2}. This is attributed to the higher moisture content of the wet BC filter cakes prior to the final heat consolidation step to produce higher grammage (25 g m^{-2} and 50 g m^{-2}) BC nanopapers, which aided the slippage and repositioning of the BC nanofibres, improving the packing efficiency of the nanofibre network

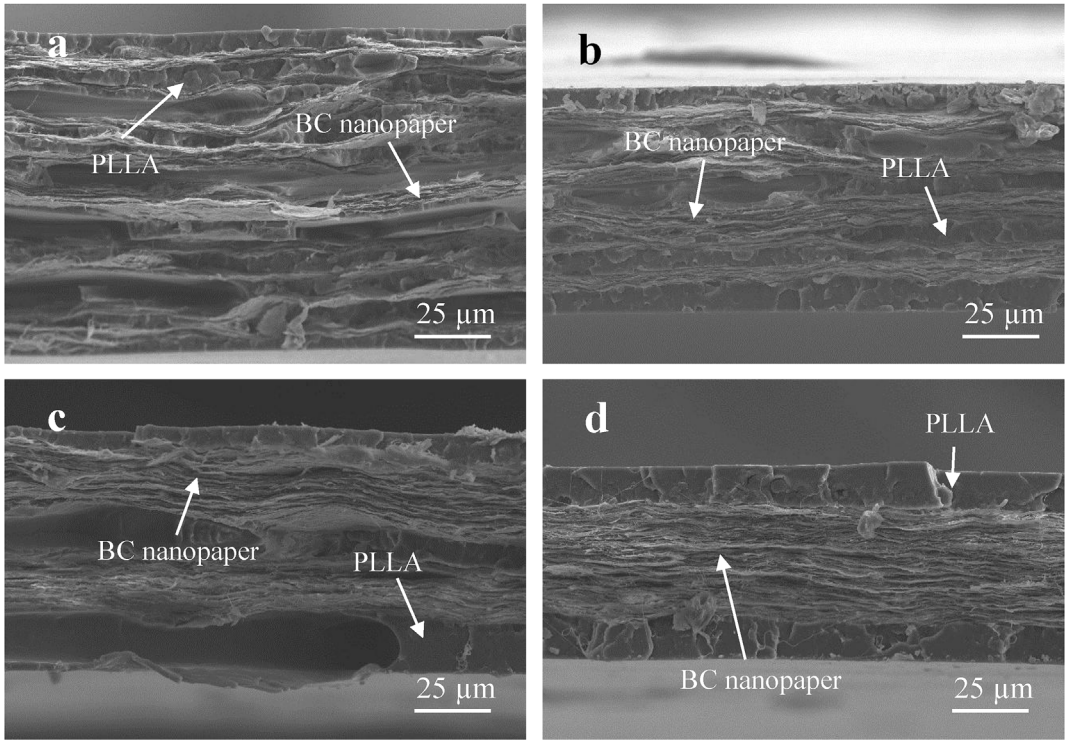

Fig. 6. Fracture surfaces of (a) Laminate **1** - consisting of 10 × 5 g m^{-2} BC nanopapers, (b) Laminate **2** - consisting of 5 × 10 g m^{-2} BC nanopapers, (c) Laminate **3** - consisting of 2 × 25 g m^{-2} BC nanopapers and (d) Laminate **4** - consisting of 1 × 50 g m^{-2} BC nanopaper, respectively.

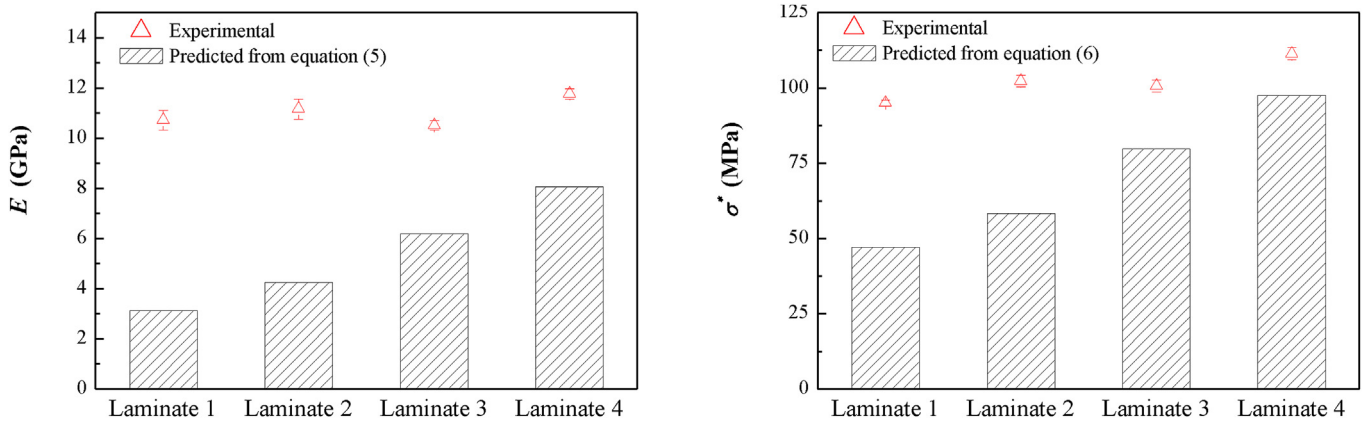

Fig. 7. Tensile modulus (E) and strength (σ^*) obtained experimentally and predicted from equations (5) and (6) for the manufactured model composite laminates.

compared to lower grammage (5 g m^{-2} and 10 g m^{-2}) BC nanopapers. In terms of the tensile properties of BC nanopapers with different grammages, both the tensile modulus (E) and tensile strength (σ^*) of the BC nanopapers decreased with decreasing nanopaper grammage; E = 2.4 GPa and σ^* = 31 MPa for 5 g m^{-2} BC nanopaper, E = 5.0 GPa and σ^* = 59 MPa for 10 g m^{-2} BC nanopaper, E = 8.9 GPa and σ^* = 104 MPa for 25 g m^{-2} BC nanopaper, and E = 12.2 GPa and σ^* = 134 MPa for 50 g m^{-2} BC nanopaper. This grammage dependency of tensile properties of BC nanopapers can be ascribed to better stress transfer efficiency of the BC nanofibres within the nanopaper when the grammage was increased.

Model BC nanopaper-reinforced PLLA composite laminates reinforced with $10 \times 5\,g\,m^{-2}$, $5 \times 10\,g\,m^{-2}$, $2 \times 25\,g\,m^{-2}$ and $1 \times 50\,g\,m^{-2}$ sheet(s) of BC nanopaper, respectively, were also manufactured. Overall, the model BC nanopaper-reinforced PLLA composite laminates possessed E = 10.5–11.8 GPa and σ^* = 95.0–11.4 MPa, respectively, at a $v_{f,BC}$ = 39–53 vol.-%, independent of the grammage of the reinforcing BC nanopaper and its measured tensile properties. This contradicts with the prediction of the tensile properties of cellulose nanopaper-reinforced polymer composites based on the volume-weighted average between the tensile properties of the reinforcing cellulose nanopaper and the polymer matrix. It was found that the porosity of the model BC nanopaper-reinforced PLLA composite laminates were significantly lower than their theoretical porosities that was calculated based on the assumption that BC nanopaper are incompressible and impermeable to molten PLLA. This suggests that the heat consolidation of molten PLLA and BC nanopapers led to the impregnation of the surface porosity of the BC nanopaper, which was not taken into account by the prediction of the tensile properties of cellulose nanopaper-reinforced polymer composites based on the volume-weighted average between the tensile properties of the reinforcing cellulose nanopaper and the polymer matrix.

Acknowledgments

The authors would like to thank the UK Engineering and Physical Science Research Council (EPSRC) for funding this work (EP/M012247/1) and the Department of Aeronautics of Imperial College London for funding MH.

References

[1] K.-Y. Lee, Y. Aitomäki, L.A. Berglund, K. Oksman, A. Bismarck, On the use of nanocellulose as reinforcement in polymer matrix composites, Compos. Sci. Technol. 105 (2014) 15–27.
[2] A. Dufresne, Cellulose nanomaterial reinforced polymer nanocomposites, Curr. Opin. Colloid Interface Sci. 29 (2017) 1–8.
[3] Y. Habibi, Key advances in the chemical modification of nanocelluloses, Chem. Soc. Rev. 43 (2014) 1519–1542.
[4] I.A. Sacui, R.C. Nieuwendaal, D.J. Burnett, S.J. Stranick, M. Jorfi, C. Weder, E.J. Foster, R.T. Olsson, J.W. Gilman, Comparison of the properties of cellulose nanocrystals and cellulose nanofibrils isolated from bacteria, tunicate, and wood processed using acid, enzymatic, mechanical, and oxidative methods, ACS Appl. Mater. Interfaces 6 (2014) 6127–6138.
[5] D. Klemm, F. Kramer, S. Moritz, T. Lindstrom, M. Ankerfors, D. Gray, A. Dorris, Nanocelluloses: a new family of nature-based materials, Angew Chem. Int. Ed. Engl. 50 (2011) 5438–5466.
[6] K.-Y. Lee, J.J. Blaker, R. Murakami, J.Y.Y. Heng, A. Bismarck, Phase behavior of medium and high internal phase water-in-oil emulsions stabilized solely by hydrophobized bacterial cellulose nanofibrils, Langmuir 30 (2014) 452–460.
[7] L. Heath, W. Thielemans, Cellulose nanowhisker aerogels, Green Chem. 12 (2010) 1448–1453.
[8] F.W. Herrick, R.L. Casebier, J.K. Hamilton, K.R. Sandberg, A. Sarko (Ed.), Microfibrillated Cellulose: Morphology and Accessibility, Wiley, 1983, pp. 797–813.
[9] A.F. Turbak, F.W. Snyder, K.R. Sandberg, Microfibrillated cellulose, a new cellulose product: properties, uses, and commercial potential, Appl. Polym. Symp. 37 (1983) 815–827.
[10] G. Siqueira, J. Bras, A. Dufresne, Cellulose whiskers versus microfibrils: influence of the nature of the nanoparticle and its surface functionalization on the thermal and mechanical properties of nanocomposites, Biomacromolecules 10 (2009) 425–432.
[11] T. Taniguchi, K. Okamura, New films produced from microfibrillated natural fibres, Polym. Int. 47 (1998) 291–294.
[12] O. Nechyporchuk, M.N. Belgacem, J. Bras, Production of cellulose nanofibrils: a review of recent advances, Ind. Crop. Prod. 93 (2016) 2–25.
[13] K.Y. Lee, G. Buldum, A. Mantalaris, A. Bismarck, More than meets the eye in bacterial cellulose: biosynthesis, bioprocessing, and applications in advanced fiber composites, Macromol. Biosci. 14 (2014) 10–32.
[14] P. Lahtinen, S. Liukkonen, J. Pere, A. Sneck, H. Kangas, A comparative study of fibrillated fibers from different mechanical and chemical pulps, BioResources 9 (2014) 2115–2127.
[15] M. Henriksson, L.A. Berglund, Structure and properties of cellulose nanocomposite films containing melamine formaldehyde, J. Appl. Polym. Sci. 106 (2007) 2817–2824.
[16] Y. Aitomäki, S. Moreno-Rodriguez, T.S. Lundström, K. Oksman, Vacuum infusion of cellulose nanofibre network composites: influence of porosity on permeability and impregnation, Mater. Des. 95 (2016) 204–211.
[17] A.N. Nakagaito, S. Iwamoto, H. Yano, Bacterial cellulose: the ultimate nano-scalar cellulose morphology for the production of high-strength composites, Appl. Phys. Mater. Sci. Process 80 (2005) 93–97.
[18] T. Montrikittiphant, M. Tang, K.Y. Lee, C.K. Williams, A. Bismarck, Bacterial cellulose nanopaper as reinforcement for polylactide composites: renewable thermoplastic nanopapreg, Macromol. Rapid Commun. 35 (2014) 1640–1645.
[19] K.-Y. Lee, T. Tammelin, K. Schulfter, H. Kiiskinen, J. Samela, A. Bismarck, High performance cellulose nanocomposites: comparing the reinforcing ability of bacterial cellulose and nanofibrillated cellulose, ACS Appl. Mater. Interfaces 4 (2012) 4078–4086.
[20] M. Nogi, S. Iwamoto, A.N. Nakagaito, H. Yano, Optically transparent nanofiber paper, Adv. Mater. 21 (2009) 1595–1598.
[21] L. Zhang, W. Batchelor, S. Varanasi, T. Tsuzuki, X. Wang, Effect of cellulose nanofiber dimensions on sheet forming through filtration, Cellulose 19 (2012) 561–574.
[22] M. Hervy, A. Santmarti, P. Lahtinen, T. Tammelin, K.-Y. Lee, Sample geometry dependency on the measured tensile properties of cellulose nanopapers, Mater. Des. 121 (2017) 421–429.
[23] F.W. Brodin, Ø. Eriksen, Preparation of individualised lignocellulose microfibrils based on thermomechanical pulp and their effect on paper properties, Nord. Pulp Pap Res. J. 30 (2015) 443–451.
[24] M. Iguchi, S. Yamanaka, A. Budhiono, Bacterial cellulose—a masterpiece of nature's arts, J. Mater. Sci. 35 (2000) 261–270.
[25] S. Gea, F.G. Torres, O.P. Troncoso, C.T. Reynolds, F. Vilasecca, M. Iguchi, T. Peijs, Biocomposites based on bacterial cellulose and apple and radish pulp, Int. Polym.

Process. 22 (2007) 497–501.
[26] F. Quero, S.J. Eichhorn, M. Nogi, H. Yano, K.-Y. Lee, A. Bismarck, Interfaces in cross-linked and grafted bacterial cellulose/poly(lactic acid) resin composites, J. Polym. Environ. 20 (2012) 916–925.
[27] A. Vainio, H. Paulapuro, Interfiber bonding and fiber segment activation in paper, BioResources 2 (2007) 442–458.
[28] W.H. Burgess, Effect of basis weight on tensile strength, TAPPI J. 53 (1970) 1680–1682.
[29] R.S. Seth, J.T. Jantunen, C.S. Moss, The effect of grammage on sheet properties, Appita 42 (1989) 42–48.
[30] S.J. Eichhorn, W.W. Sampson, Statistical geometry of pores and statistics of porous nanofibrous assemblies, J. R. Soc. Interface R. Soc. 2 (2005) 309–318.
[31] S.J. I'Anson, W. Sampson, S. Savani, Density dependent influence of grammage on tensile properties of handsheets, J. Pulp Pap. Sci. 34 (2008) 182–189.
[32] X. Xu, J. Zhou, L. Jiang, G. Lubineau, T. Ng, B.S. Ooi, H.-Y. Liao, C. Shen, L. Chen, J.Y. Zhu, Highly transparent, low-haze, hybrid cellulose nanopaper as electrodes for flexible electronics, Nanoscale 8 (2016) 12294–12306.